
Seeing 3D Objects in a Single Image via Self-Supervised Static-Dynamic Disentanglement

Prafull Sharma^{1*}Ayush Tewari¹Yilun Du¹Sergey Zakharov⁴Rares Ambrus⁴Adrien Gaidon⁴William T. Freeman¹Frédo Durand¹Joshua B. Tenenbaum^{1,2,3}Vincent Sitzmann¹

¹MIT CSAIL ²MIT BCS ³MIT CBMM ⁴Toyota Research Institute
prafullsharma.net/see3d

Abstract

Human perception reliably identifies movable and immovable parts of 3D scenes, and completes the 3D structure of objects and background from incomplete observations. We learn this skill not via labeled examples, but simply by observing objects move. In this work, we propose an approach that observes unlabeled multi-view videos at training time and learns to map a single image observation of a complex scene, such as a street with cars, to a 3D neural scene representation that is disentangled into movable and immovable parts while plausibly completing its 3D structure. We separately parameterize movable and immovable scene parts via 2D neural ground plans. These ground plans are 2D grids of features aligned with the ground plane that can be locally decoded into 3D neural radiance fields. Our model is trained self-supervised via neural rendering. We demonstrate that the structure inherent to our disentangled 3D representation enables a variety of downstream tasks in street-scale 3D scenes using simple heuristics, such as extraction of object-centric 3D representations, novel view synthesis, instance segmentation, and 3D bounding box prediction, highlighting its value as a backbone for data-efficient 3D scene understanding models. This disentanglement further enables scene editing via object manipulation such as deletion, insertion, and rigid-body motion.

1 Introduction

Parsing a scene into movable objects and immovable background is a critical aspect of visual perception. Humans succeed at this task given just a single, static image. Furthermore, our perception is not restricted to 2D, as we are capable of forming a belief over the 3D geometry of the *occluded* parts of objects, such as a mug or a car, given a partial observation from only a single viewpoint. These fundamental skills of scene understanding are largely self-supervised, and learned simply by moving in and interacting with our 3D environment. In this work, we present a self-supervised approach which aims to solve the same problem by learning to reconstruct representations of 3D scenes that disentangle static background from movable objects, while completing occluded regions. Inspired by research on human perception that suggests that motion is a critical cue to learn our prior for object discovery, we leverage motion as an objectness cue and train on multi-view videos. At test time, our model can reconstruct disentangled 3D representations from just a single static image.

*Email: prafull@mit.edu, vsitzmann@mit.edu

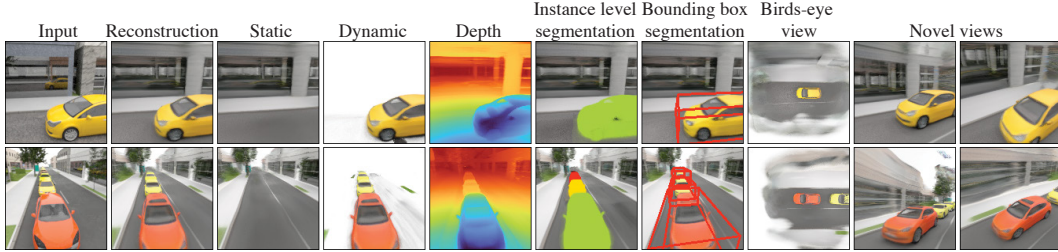


Figure 1: Given a single image, our model infers separate 3D representations for static and dynamic scene elements, enabling high-quality novel view synthesis with plausible completion, unsupervised instance segmentation, 3D bounding box prediction, 3D scene editing, and the extraction of object-centric 3D representations. Our model is trained self-supervised using unlabeled multi-view video.

Recent work in self-supervised learning has made significant progress towards the goal of object discovery via self-supervised object-centric representation learning for images [1, 2] and videos [3]. These methods segment an image or video into non-overlapping objects and infer a latent code for each of them, however, they are either constrained to simple toy environments, or require video with additional annotations, such as bounding boxes, at test time. The resulting object-centric latent codes can be decoded into object-centric 3D scene representations [4–6]. Here, 3D notions, such as 3D scale and connectedness, can serve as additional training signal, but methods are similarly limited to simple scenes. Our work is further inspired by recent work on learning 3D representations of dynamic scenes [7–9]. While most of these approaches are focused on high-quality novel-view synthesis, a few also enable disentanglement of static and dynamic components [10, 11]. However, most of these approaches are overfit to a single scene, and can thus only disentangle movable and immovable scene parts in that single scene, without acquiring knowledge about objectness that generalizes across scenes. They further do not support inference from partial observations, such as a single image.

In this work, we propose an approach that learns to map a single image to a 3D neural scene representation that is disentangled into static background and movable object 3D representations. Specifically, given a single image, our model infers a *neural ground plan*, a 2D grid of learned features aligned with the ground plane. Continuous 3D points may be decoded for volume rendering by projecting them onto the ground plan, retrieving the respective features, and decoding them via an MLP. By observing multi-view video at training time, our model learns an objectness prior that, at test time, enables it to map a single image observation to separate static “background” and movable “object” ground plans. Our model is trained self-supervised via neural rendering, without pseudo-ground truth, bounding boxes, or any instance labels.

Neural ground plans exploit the fact that in scenes with physical objects moving mostly under their own power, such as streets with cars, pedestrians, and bicyclists, as a consequence of gravity, most objects move on the 2D ground plane. Here, neural ground plans offer a dense, yet memory-efficient neural scene representation. Ground plans have been shown to be effective 3D representation in robotics and autonomous driving applications [12], as well as in computer graphics for unconditional synthesis of indoor scenes [13]. Our method shows how we can reconstruct disentangled neural ground plans from monocular images of unbounded scenes using self-supervised learning via neural rendering. We demonstrate that our model enables instance segmentation, recovery of 3D object-centric representations, and 3D bounding box prediction via a simple heuristic leveraging that connected regions of 3D space that move together belong to the same object. The proposed representation also enables intuitive editing of the scenes using manipulation of individual objects. On a dataset of high-quality renderings of street-scale scenes, our model outperforms prior pixel-aligned approaches in novel view synthesis fidelity as well as prior work on the self-supervised discovery of object-centric 3D representations in terms of object discovery. In summary, our contributions are:

- We introduce self-supervised training of conditional neural ground plans, a hybrid discrete-continuous 3D neural scene representation that can be reconstructed from a single image, enabling efficient processing of scene appearance and geometry directly in 3D.
- We leverage object motion as a cue to learn to disentangle static background and movable foreground objects given only a single input image.

- Using a simple hand-crafted heuristic, our structured neural scene representation enables strong single-image 3D instance segmentation and 3D bounding box prediction, demonstrating its value as a backbone for data-efficient prior-based 3D processing.

2 Related Work

Neural Scene Representation and Rendering. Several works have explored learning neural scene representations for downstream tasks in 3D. Earlier approaches used voxel grids as the 3D representation [14, 15]. However, voxel grids are memory intensive, and thus, it is difficult to scale these methods to high resolutions. Emerging neural scene representations enable self-supervised reconstruction of geometry and appearance at high-resolutions given only image observations. A large part of recent work focuses on the case of reconstructing a *single* 3D scene given dense observations [16–20], enabling high-quality novel view synthesis with exciting applications in computer graphics. Alternatively, differentiable neural rendering may be used to supervise encoders to enable 3D reconstruction from incomplete image observations [21–30]. Fu and Zhang et al. [31] use neural rendering as a tool to recover high-quality 2D panoptic segmentation annotations from a set of sparse images and noisy 3D bounding primitives and 2D predictions. Hybrid discrete-continuous neural scene representations enable faster rendering [32–36]. Neural ground plans and axis-aligned 2D grids enable high-quality unconditional generation of 3D scenes [13, 32]. Axis-aligned feature grids have also been used for reconstruction of 3D geometry from pointclouds [37]. We similarly use axis-aligned 2D grids of features for self-supervised scene representation via neural rendering, but reconstruct them directly from few or a single 2D image observations.

Birds-Eye View Representations. Birds-eye view has been explored as a 3D representation in robotics, particularly for autonomous driving applications. Prior work uses ground-plane 2D grids as representations for object detection and segmentation [12, 38–41], layout generation and completion [42–45], and next-frame prediction [46, 47]. The birds-eye view is generated either directly without 3D inductive biases [44], or similar to our proposed approach, by using 3D geometry-driven inductive biases such as unprojection into a volume [38, 48, 41], or by generating a 3D point cloud [39, 46]. However, prior approaches are supervised, using ground truth bounding boxes or semantic segmentation as supervision. In contrast, we present the first self-supervised conditional ground plan representation, learned only from posed images via neural rendering. While we show that our self-supervised representation can be used for rich inference tasks using simple heuristics, our method may be extended for more challenging tasks using the techniques developed in prior work.

Dynamic-Static Disentanglement. Our work is related to prior art on learning to disentangle dynamic objects and static background. Some prior work leverages object motion across video frames to learn separate representations for movable foreground and static background in 2D [49–51], while other recent work can also learn 3D representations [10, 11]. Our approach is similar in using object motion as cue for disentanglement and multi-view as cue for 3D reconstruction, but uses it as supervision to train an encoder-based approach that enables reconstruction from a *single* image instead of scene-specific disentanglement from multiple video frames.

Object-centric Scene Representations. Prior work has aimed to infer object-centric representations directly from images, with objects either represented as localized object-centric patches [52–56] or scene mixture components [2, 57–61], with the slot attention module [1] increasingly driving object-centric inference. Resulting object representations may be decoded into object-centric 3D representations and composed for novel view synthesis [4, 6, 62–68]. BlockGAN and GIRAFFE [69, 70] build unconditional generative models for compositions of 3D-structured representations, but only tackle generation, not reconstruction. Some methods rely on annotations such as bounding boxes, object classes, 3D object models, or instance segmentation to recover object-centric neural radiance fields [71–74]. Several scene reconstruction methods [65–67, 75] use direct supervision to train an object representation and detector to infer an editable 3D scene from a single frame observation. Kipf et al. [3] leverage motion as a cue for self-supervised object disentanglement, but do not reconstruct 3D and require additional conditioning in the form of bounding boxes. We propose to reconstruct separate 3D representations of movable objects and static background in 3D *prior* to inferring object-centric representations. This drastically simplifies object discovery, and we demonstrate that a simple heuristic is sufficient to perform discovery of object-centric representations in street-scale scenes. However, we highlight that our work is *complimentary* to the work discussed

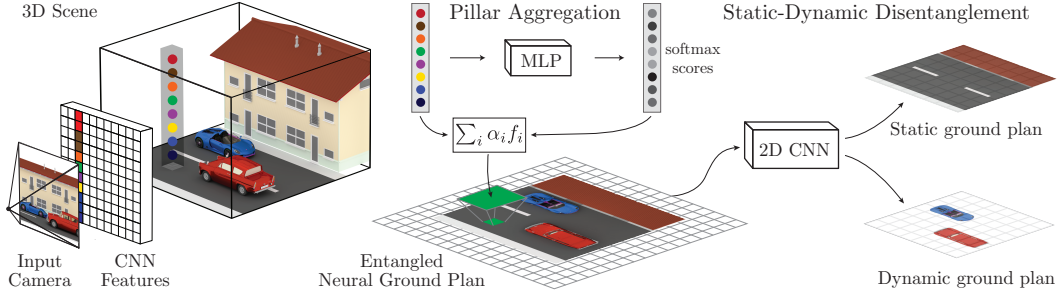


Figure 2: **Ground plan inference.** Given a context image, we first extract a set of CNN features. We unproject the features into 3D and re-sample them at “pillars” on top of the location of ground plan vertices. Pillars are aggregated into ground plan features using a softmax-weighted sum. The resulting 2D grid of features is decomposed into separate dynamic and static ground plans by a 2D CNN. The coordinate-encoding MLP is not visualized in this figure. Please refer to Sec. 3 for details.

here: slot attention and related object-centric algorithms can be run on our already sparse ground plan of movable 3D regions, faced with a dramatically easier task than when run on images directly.

3 Conditional Neural Ground Plans

We introduce conditional neural ground plans as a hybrid discrete-continuous scene representation for 3D scene understanding, reconstructed from single images and trained via multi-view video. We first describe the case without static-dynamic disentanglement (“Entangled Neural Ground Plan” in Fig. 3), which we will discuss in the next section. Please see Fig. 2 for an illustration of the reconstruction of a neural ground plan from a single image.

Compactified neural ground plans for unbounded scene representations. A neural ground plan is a 2D grid of features aligned with the ground plane of the 3D scene, which we define to be the xz -plane. A 3D point is decoded by projecting it onto the ground plan and retrieving the corresponding feature vector using bilinear interpolation. This feature is then concatenated with the vertical y -coordinate of the query point and decoded into radiance and density values via a fully connected network, enabling novel view synthesis using volume rendering. In this definition, however, it is only possible to decode 3D points that lie within the boundaries of the neural ground plan, which precludes reconstruction and representation of unbounded scenes. We thus compactify \mathbb{R}^2 by implementing a non-linear coordinate re-mapping as proposed in [76]. xz -coordinates within a radius r_{inner} around the ground plan origin remain unaffected, but xz -coordinates of points outside this radius are contracted. For any point $\mathbf{p} \in \mathbb{R}^2$ on the ground plan, the contracted coordinate can be computed as $\mathbf{p}' = ((1+k) - k/\|\mathbf{u}\|)(\mathbf{u}/\|\mathbf{u}\|)r_{\text{inner}}$, where $\mathbf{u} = \mathbf{p}/r_{\text{inner}}$, and k is a hyperparameter which controls the size of the contracted region.

Assumptions and benefits. Parameterizing the scene as 2D neural ground plans has several advantages over alternative scene representations. Compared to parameterizing the entire scene as a single, monolithic MLP, rendering is significantly cheaper, as in other hybrid discrete-continuous neural fields [77]. Note that while it is possible for a feature to parameterize more than one object per tile, it is difficult to reconstruct stacks of *unseen* numbers of objects. When reasoning about dynamics, the neural ground plan encodes an inductive bias that most motion happens in the ground plane. In applications such as self-driving, a ground plan is an appropriate memory-efficient representation. For other tasks, such as stacking of boxes, it is prudent to expand the ground plan to a voxel grid along the y -axis. A core benefit of both voxel grids and ground plans as 3D representations is that they enable shift-equivariant processing of the 3D scene via convolutions, without concern for occlusions and perspective distortion, and enable straight-forward editing of the 3D scene.

Reconstructing neural ground plans from images. Inferring a neural ground plan from one or several images proceeds in three steps: (1) feature extraction, (2) feature unprojection, (3) pillar aggregation. Given a single image \mathbf{I} , we first extract per-pixel features via a CNN encoder to yield a feature tensor \mathbf{F} . We define the camera as the world origin and center the neural ground plan accordingly, approximately aligned with the ground level. We unproject the image features along their respective rays as parameterized via the intrinsic and extrinsic camera parameters to create a

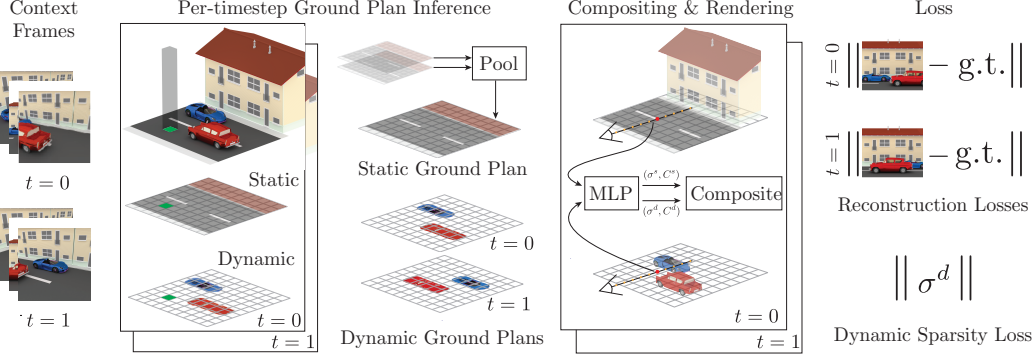


Figure 3: **Learning Static-Dynamic Disentanglement.** Given multiple frames of a video, we extract per-frame, compactified static and dynamic ground plans according to Fig. 2. Static ground plans are pooled into a time-invariant ground plan. We then composite per-frame dynamic and static time-invariant ground plans via differentiable volume rendering. Our model is supervised only via a re-rendering loss on video frames. We encourage the model to explain as much of the scene density as possible with the static ground plan via a sparsity loss on per-frame dynamic volume rendering densities. The surface loss is not visualized here.

discrete volume in the world space \mathbf{v} , where $\mathbf{v}(\mathbf{x}) = \mathbf{F}(\pi(\mathbf{x}))$ at a 3D grid point \mathbf{x} on the volume, and $\pi(\cdot)$ is the projection operation. The xz -coordinates of this volume are aligned with our ground plan representation. At any vertex of the ground plan, the discretized y -coordinates of the volume form a “pillar”. The next steps will aggregate each pillar into a point in order to create the 2D ground plan. We first use a coordinate-encoding MLP to transform the volume as $\mathbf{f}(\mathbf{x}) = D(\mathbf{v}(\mathbf{x}), \mathbf{x}_c, \mathbf{d})$, where the function $D(\cdot)$ denotes the MLP, \mathbf{x}_c denotes the camera-space coordinates of the 3D grid point, and \mathbf{d} denotes the ray direction from the camera center to \mathbf{x} . Since all features along a camera ray are identical in \mathbf{v} , coordinate encoding is used to add the depth information to the features. If we have access to multi-view input images, the volumes corresponding to each input view are mean pooled at this point. Associated with each 2D vertex of the ground plan is now a set of features $\{\mathbf{f}_i\}_{i=1}^N$, where N is the length of the y -dimension in the volume. We use a pillar-aggregation MLP to compute softmax scores as $\alpha_i = P(\mathbf{f}_i, \mathbf{x}_i)$, where $P(\cdot)$ denotes the MLP and \mathbf{x}_i is the coordinate of the i -th point on the pillar. Finally, the features are aggregated as $\mathbf{g} = \sum_i \alpha_i \mathbf{f}_i$.

Differentiable Rendering. We can render images from novel camera views via differentiable volume rendering [13, 17, 18]. To resolve points closer to the camera more finely, we adopt logarithmic sampling of points along the ray with more samples close to the camera [78]. For each sampled point \mathbf{x} on the camera ray, we need to compute its density and color for volume rendering. This is accomplished using a rendering MLP, as $(\mathbf{c}_x, \sigma_x) = R(\mathbf{g}_x, y_x)$, where $R(\cdot)$ denotes the MLP, \mathbf{g}_x are the ground plan features for the point \mathbf{x} computed by projecting the coordinates onto the ground plane and bilinearly interpolating the nearest grid points, and y_x is the height at the projected point on the ground plane. The rendering MLP enables a full 3D reconstruction using the ground plan.

4 Learning Static-Dynamic Disentanglement

We now describe how motion over time is leveraged to disentangle dynamic and static scene parts, and how we use the resulting scene representation for self-supervised 3D object discovery and 3D bounding box prediction in street scenes via a simple heuristic. Please see Fig. 3 for an overview of the multi-frame training for dynamic-static disentanglement.

Disentangling static and dynamic neural ground plans. We leverage multi-view *video* as the training signal. We pick two frames of a video. For each frame, we infer an *entangled* neural ground plan as described in the previous section. Features in this entangled neural ground plan parameterize both static and dynamic features of the scene, for instance, a car as well as the road below it. We feed this ground plan into a fully convolutional 2D network, which disentangles it into two separate ground plans containing *dynamic* and *static* features. The per-frame static ground plans are pooled to obtain a single, time-independent static ground plan.

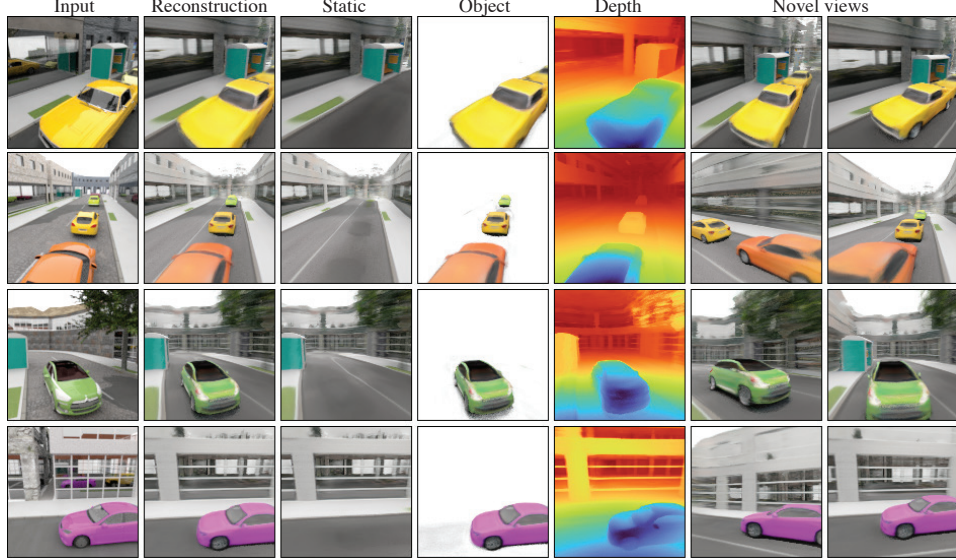


Figure 4: **Single-image reconstruction, disentanglement of static and dynamic objects, and novel view synthesis.** Given a single input image, our method can disentangle the observed scene into static and object components based on what the model observed as not-moving and moving in the training data. In these examples, the cars are isolated in the object component as the model was training on video data of cars moving on the road.

The xz -coordinates in the entangled ground plan are linearly spaced. The CNN also transforms the ground plans to the *compactified* \mathbb{R}^2 space as explained earlier. Vertices in this compactified space are arranged on regular grids close to the camera and grow increasingly sparse with increasing distance. Note that a 2D CNN in the ground plan space is a 3D operation, since ground plans implicitly parameterize 3D scene representations.

Compositing ground plans. To render a scene disentangled into static and dynamic ground plans, we first decode query points using both ground plans, yielding *two* sets of (density, color) values for each point. We now follow STaR [10] to compose the contribution from static and dynamic components along the ray. Given the color and density for static (\mathbf{c}^S, σ^S) and dynamic (\mathbf{c}^D, σ^D) parts, the density of the combined scene is calculated as $\sigma^S + \sigma^D$. The color at the sampled point is computed as a weighted linear combination $w^S \mathbf{c}^S + w^D \mathbf{c}^D$, where $w^S = (1 - \exp(-\delta\sigma^S))/(1 - \exp(-\delta(\sigma^S + \sigma^D)))$, $w^D = (1 - \exp(-\delta\sigma^D))/(1 - \exp(-\delta(\sigma^S + \sigma^D)))$, and δ is the distance between adjacent samples on the camera ray.

Losses and Training. We train our model on multi-view video, where multi-view information is used to learn 3D structure, while motion is used to disentangle the static and dynamic components in the scene. During training, we sample two time-steps per video. For each time-step, we sample multiple images from different camera views; some of the views are used as input to the method while others are used to compute the loss function. We use the input images to infer static and dynamic ground plans, and use them to render out per-frame query views. Our per-frame loss consists of an image reconstruction term, a hard surface constraint, and a sparsity term.

$$\mathcal{L} = \underbrace{\|R - I\|_2^2 + \lambda_{\text{LPIPS}} \mathcal{L}_{\text{LPIPS}}(R, I)}_{\mathcal{L}_{\text{img}}} - \underbrace{\lambda_{\text{surface}} \sum_i \log(\mathbb{P}(w_i))}_{\mathcal{L}_{\text{surface}}} + \underbrace{\lambda_{\text{sparse}} \sum_i |\sigma_i^D|}_{\mathcal{L}_{\text{dyn_sparsity}}}. \quad (1)$$

\mathcal{L}_{img} measures the difference between the rendered and ground truth images, R and I respectively, using a combination of ℓ_2 and patch-based LPIPS perceptual loss. $\mathcal{L}_{\text{surface}}$ encourages both static and dynamic weight values (the weight for each sample in the rendering equation) w_i for all samples along the rendered rays to be either 0 or 1, encouraging hard surfaces [79]. Here, $\mathbb{P}(w_i) = \exp(-|w_i|) + \exp(-|1 - w_i|)$. The sparsity term $\mathcal{L}_{\text{dyn_sparsity}}$ takes as input densities decoded from the dynamic ground plan from all rendered rays, and encourages the values to be sparse. This forces the model to explain as much non-empty 3D structure as possible via the static ground plan, leading to reliable

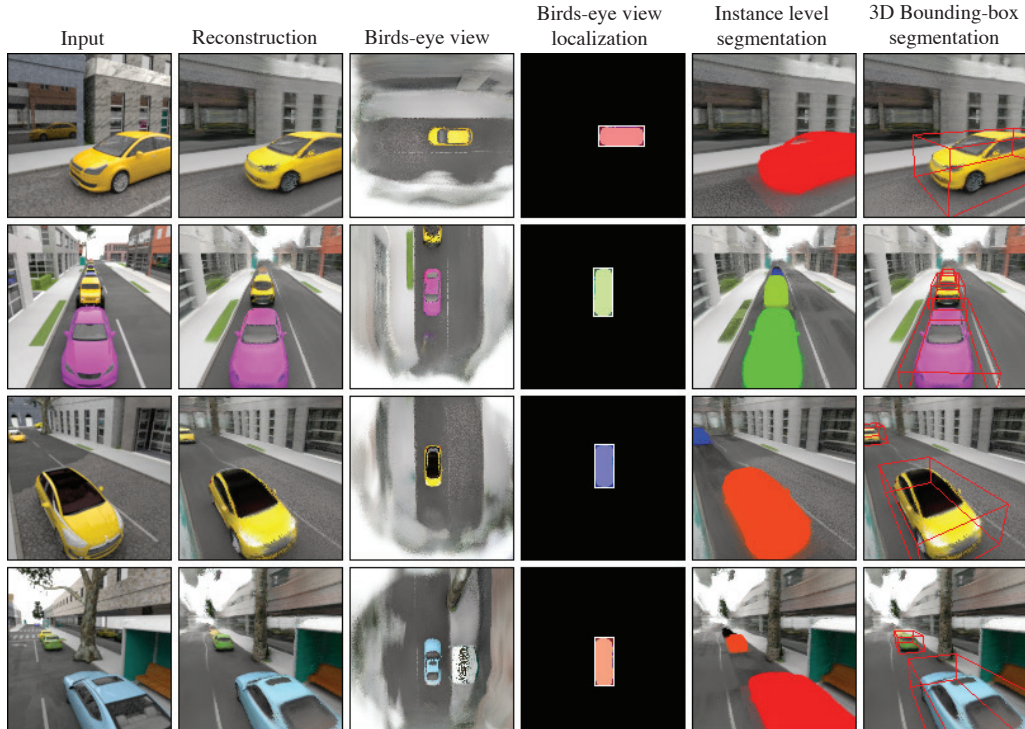


Figure 5: **Localization of objects:** Given a single input image, we can use our inferred 3D representation of the scene to compute (a) birds-eye view rendering, (b) object localization in the birds-eye view space, (c) instance-level segmentation, and (d) 3D bounding box prediction.

static-dynamic disentanglement. Without this loss, the model could explain the entire scene with just the dynamic component. The loss functions are weighed using the hyperparameters λ_{LPIPS} , λ_{surface} and λ_{sparse} . While we describe the loss functions for a single sample of ground-truth and rendered image, in practice, we construct mini-batches by randomly choosing multiple views of a scene at different time steps, and evaluate the loss function on each sample.

Unsupervised object detection and extracting object-centric 3D representations. Our formulation yields a model that maps a single image to two radiance fields, parameterizing static and dynamic 3D regions respectively. Please see Fig. 1 for an example. We now perform a simple search for connected components in the dynamic neural ground plan, performing *unsupervised* 3D instance segmentation, monocular 3D bounding box prediction, and the extraction of object-centric 3D representations. Specifically, given a dynamic ground plan, we first sample points in a 3D grid around the ground plan origin and decode their densities. We now perform conventional connected-component labeling in the ground plane space using accumulated density values, identifying disconnected dynamic objects. Using volume rendering, we can perform screen-space instance segmentation, see Fig. 1 for an example. 3D bounding boxes for each instance can be extracted by recovering the smallest box containing some percentage of the total density of the connected component. Finally, we may simply crop tiles of the dynamic ground plan that belong to a given object instance, yielding object-centric 3D representations, enabling editing of 3D scenes such as deletion, insertion, and rigid-body transformation of objects. This approach is not limited to a fixed number of objects during training or at test time. As we will show, this simple method is at-par with the state of the art on self-supervised learning of object-centric 3D representations, uORF [4]. However, this simple heuristic is not capable of segmenting objects that are *in physical contact*. In self-driving scenarios, this is of limited concern, but in general 3D scenes, this assumption is regularly violated. Note that our approach is *entirely compatible* with prior work leveraging slot attention [1, 3] and other inference modules, which can simply be run on the disentangled dynamic ground plan, which guarantees a structured and sparse semantic space that drastically simplifies instance segmentation.

Table 1: Quantitative baseline comparison of novel view synthesis results. We outperform PixelNeRF [22] and uORF [4] in terms of PSNR, SSIM, and LPIPS on both CLEVR and CoSY datasets.

	CLEVR (1 view)			CoSY (1 view)			CoSY (5 views)		
	PSNR \uparrow	SSIM \uparrow	LPIPS \downarrow	PSNR \uparrow	SSIM \uparrow	LPIPS \downarrow	PSNR \uparrow	SSIM \uparrow	LPIPS \downarrow
Ours	34.5	0.956	0.15	15.71	0.43	0.53	18.29	0.57	0.43
PixelNeRF	33.98	0.945	0.200	14.61	0.34	0.64	17.31	0.49	0.50
uORF	29.35	0.898	0.151	—	—	—	—	—	—

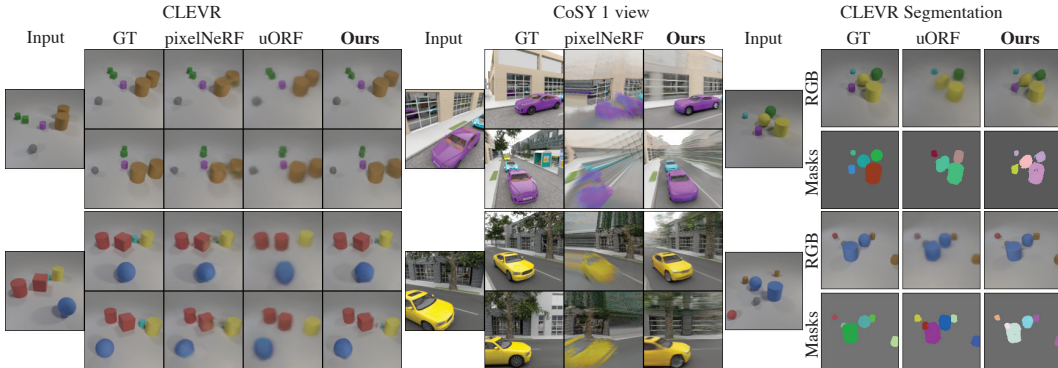


Figure 6: **Qualitative comparisons.** Left two columns: Novel-view synthesis comparison with uORF [4] and PixelNeRF [22]. Right: Instance segmentation comparison with uORF [4].

5 Results

We demonstrate that our method can reconstruct street-scale 3D scenes using just a single image observation, disentangling dynamic foreground objects and static background. Using the proposed heuristic, we show that this can be leveraged for unsupervised instance segmentation and 3D bounding box detection. Our method achieves state-of-the-art performance both in terms of novel view synthesis as well as unsupervised 3D object discovery. We also demonstrate high-quality editing of the scene via manipulation of the individual objects. We encourage readers to refer to the supplemental material for more results, including video results.

Datasets. Our method is trained on multi-view observations of dynamic scenes. To this end, we leverage CoSY [80], a procedural generator of street scenes, and render multi-view observations of 9000 scenes with moving cars, sampled using 15 background city models and 95 car models. Due to the procedural generation of the city with finite assets, different city instances use the same building geometry and textures but in different combinations. We train on 8000 scenes, and evenly split the rest into validation and test sets. We use the CLEVR dataset [4] for self-supervised object discovery benchmarks. Datasets and code will be made public.

Baselines. For single-shot 3D reconstruction and novel view synthesis, we compare against PixelNeRF [22], a state-of-the-art single-image 3D reconstruction method. For unsupervised object-centric 3D reconstruction, we compare against the state-of-the-art method uORF [4]. We train PixelNeRF models on our datasets using publicly available code. We finetune the uORF model pretrained on CLEVR on our CLEVR renderings, and train it from scratch on CoSY using publicly available code.

Single-image Static and Dynamic 3D Reconstruction. Fig. 4 shows results on single-image reconstruction of static and dynamic scene elements. Given only a single image, our method reliably segments the scene into static and dynamic parts. It plausibly completes parts of the scene that are unobserved in the context image but sufficiently constrained, such as the back-side of cars or the unobserved patch of road beneath a car. As expected from a non-generative method, regions that are entirely unconstrained such as occluded parts of the background are blurry. Fig. 6 provides a qualitative comparison to PixelNeRF and uORF in terms of single-image 3D novel view synthesis on both CoSY and CLEVR. While PixelNeRF succeeds in novel view synthesis on CLEVR, renderings on the complex CoSY dataset show significant artifacts, which may be due to the linear sampling employed by PixelNeRF.

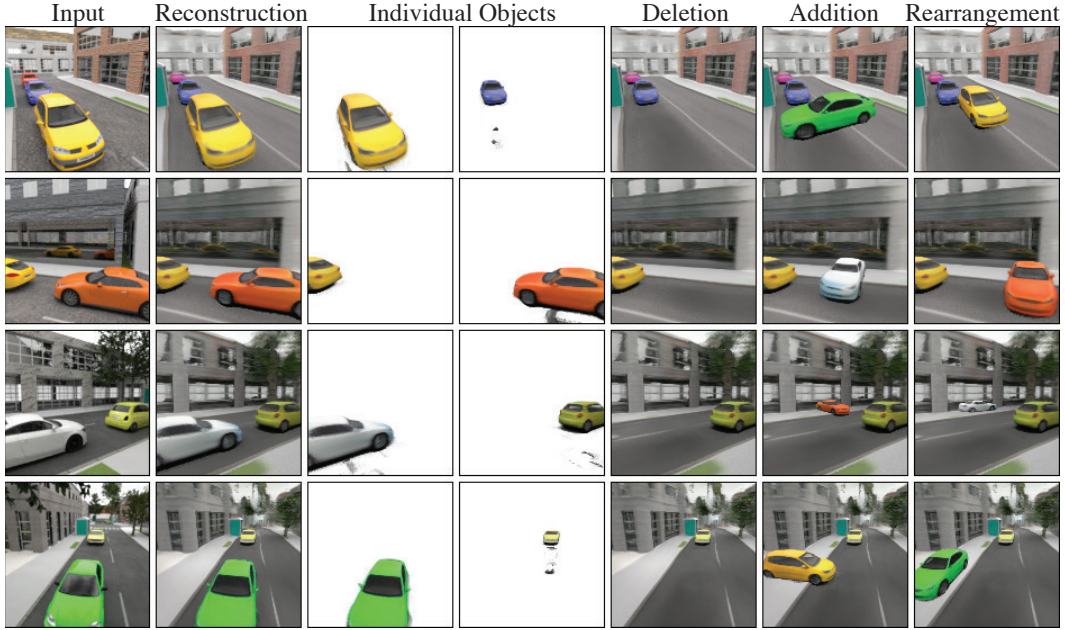


Figure 7: **Object-centric representations and scene editing.** The proposed static-dynamic neural ground plans enables object discovery using a simple heuristic of connectedness of objects (left). This enables straight-forward scene editing such as deletion, addition, or rigid-body transformation via directly editing the neural ground plan (right).

uORF does not synthesize realistic images when trained on CoSY (see supplemental for results). On CLEVR, uORF generally produces high-quality renderings, but lacks high-frequency detail. In contrast to these methods, our method reliably synthesizes novel views with high-frequency detail for both datasets, while also disentangling the scene into movable and immovable scene parts. Quantitatively, we outperform both methods on novel-view synthesis in terms of PSNR, SSIM and LPIPS metrics on both datasets, please see Table 1 for these results. Our method supports monocular 3D reconstruction, as well as multi-view reconstruction at test time. We demonstrate in Table 1 that our monocular results, while slightly lower-quality, are still comparable to reconstructions computed using 5 input views.

Seeing 3D Objects. Fig. 5 demonstrates the results of the proposed 3D object discovery heuristic based on connected dynamic component discovery in the birds-eye view, instance segmentation, and 3D bounding box prediction. Note that our method enables high-quality novel view synthesis from a birds-eye view. Fig. 6 provides a qualitative comparison of object discovery with uORF.

While uORF succeeds at segmenting CLEVR scenes with fidelity comparable to ours, it fails to provide reconstruction and instance segmentation for our diverse and visually complex street-scale CoSY dataset. Our method reliably segments separate car instances and predicts 3D bounding boxes, including for cars that are only partially observed. Table 2 quantitatively compares the computed segmentation maps on CLEVR to uORF. We use the Adjusted Rand Index (ARI) metrics following uORF. We evaluate this metric in the input view (ARI), as well as in a novel view (NV-ARI). We perform at-par with uORF on both of these metrics, demonstrating that our 3D ground plan representation reaches state of the art results with simple heuristics. In addition, as mentioned before, we achieve higher-quality novel-view synthesis results, and also achieve significantly better results on the challenging CoSY dataset. Our method is more efficient than uORF, both for training and inference. Please see the supplemental material for details.

3D Scene Editing. Fig. 7 provides editing results of our method. The instance-level segmentation, dynamic-static disentanglement, and 3D bounding boxes enable straight-forward 3D editing, such as

	ARI \uparrow	NV-ARI \uparrow
Ours	0.84	0.84
uORF	0.83	0.82

Table 2: Quantitative segmentation accuracy evaluation on CLEVR using ARI and NV-ARI metrics.

translation, rotation, deletion, and insertion of individual objects in the scene. Note that such editing is difficult with methods that lack a persistent 3D representation, such as PixelNeRF.

6 Discussion

Limitations and Future Work. Although our method achieves high-quality novel view synthesis from a single image, generated views are not photorealistic, and unobserved scene parts are blurry commensurate with the amount of uncertainty. Future work may explore plausible hallucinations of unobserved scene parts. As mentioned earlier, the heuristic employed to discover objects from the ground plan cannot identify separate objects that are in contact with each other; a limitation that could be addressed by running existing object-centric encoders [1] directly on the object ground plan. Since our model is trained on a finite set of cars and city configurations, our model does not show strong generalization to cars with out-of-distribution geometry (eg. bus, truck) and texture (eg. police car).

Ethical considerations. Our method could reduce labeling cost for tracking and detection, and poses a threat to be misused for surveillance.

Conclusion. Our paper demonstrates self-supervised learning of 3D scene representations that are disentangled into movable and immovable scene elements. While our method is trained on multi-view videos, at test time, we can reconstruct disentangled 3D representations from a single image observation. We show that neural ground plans serve as a rich representation that enable data-efficient solutions to downstream object-centric tasks such as instance segmentation, 3D bounding box prediction, and 3D scene editing. We hope that our paper will inspire future work on the use of self-supervised static-dynamic neural scene representations for general scene understanding tasks.

7 Acknowledgements and Disclosure of Funding

This work is in part supported by DARPA under CW3031624 (Transfer, Augmentation and Automatic Learning with Less Labels) and the Machine Common Sense program, Singapore DSTA under DST00OECI20300823 (New Representations for Vision), NSF CCRI # 2120095, Stanford Institute for Human-Centered Artificial Intelligence (HAI), Stanford Center for Integrated Facility Engineering (CIFE), Qualcomm Innovation Fellowship (QIF), Samsung, Ford, Amazon, and Meta. The Toyota Research Institute also partially supported this work. This article solely reflects the opinions and conclusions of its authors and not TRI or any other Toyota entity.

References

- [1] Francesco Locatello, Dirk Weissenborn, Thomas Unterthiner, Aravindh Mahendran, Georg Heigold, Jakob Uszkoreit, Alexey Dosovitskiy, and Thomas Kipf. Object-centric learning with slot attention. *Proc. NeurIPS*, 33:11525–11538, 2020.
- [2] Martin Engelcke, Adam R. Kosiorek, Oiwi Parker Jones, and Ingmar Posner. Genesis: Generative scene inference and sampling with object-centric latent representations. In *Proc. ICLR*, 2020.
- [3] Thomas Kipf, Gamaleldin F Elsayed, Aravindh Mahendran, Austin Stone, Sara Sabour, Georg Heigold, Rico Jonschkowski, Alexey Dosovitskiy, and Klaus Greff. Conditional object-centric learning from video. *arXiv preprint arXiv:2111.12594*, 2021.
- [4] Hong-Xing Yu, Leonidas J Guibas, and Jiajun Wu. Unsupervised discovery of object radiance fields. *Proc. ICLR*, 2022.
- [5] Karl Stelzner, Kristian Kersting, and Adam R Kosiorek. Decomposing 3d scenes into objects via unsupervised volume segmentation. *arXiv preprint arXiv:2104.01148*, 2021.
- [6] Cameron Smith, Hong-Xing Yu, Sergey Zakharov, Fredo Durand, Joshua B Tenenbaum, Jiajun Wu, and Vincent Sitzmann. Unsupervised discovery and composition of object light fields. *arXiv preprint arXiv:2205.03923*, 2022.
- [7] Keunhong Park, Utkarsh Sinha, Jonathan T. Barron, Sofien Bouaziz, Dan B Goldman, Steven M. Seitz, and Ricardo Martin-Brualla. Nerfies: Deformable neural radiance fields. *Proc. ICCV*, 2021.
- [8] Zhengqi Li, Simon Niklaus, Noah Snively, and Oliver Wang. Neural scene flow fields for space-time view synthesis of dynamic scenes. In *Proc. CVPR*, pages 6498–6508, 2021.
- [9] Edgar Tretschk, Ayush Tewari, Vladislav Golyanik, Michael Zollhöfer, Christoph Lassner, and Christian Theobalt. Non-rigid neural radiance fields: Reconstruction and novel view synthesis of a dynamic scene from monocular video. In *Proc. ICCV. IEEE*, 2021.
- [10] Wentao Yuan, Zhaoyang Lv, Tanner Schmidt, and Steven Lovegrove. Star: Self-supervised tracking and reconstruction of rigid objects in motion with neural rendering. In *Proc. CVPR*, pages 13144–13152, 2021.
- [11] Vadim Tschernezki, Diane Larlus, and Andrea Vedaldi. Neurdiff: Segmenting 3d objects that move in egocentric videos. In *Proc. 3DV*, pages 910–919. IEEE, 2021.
- [12] Avishkar Saha, Oscar Mendez, Chris Russell, and Richard Bowden. Translating images into maps. In *Proc. ICRA*, 2022.
- [13] Terrance DeVries, Miguel Angel Bautista, Nitish Srivastava, Graham W. Taylor, and Joshua M. Susskind. Unconstrained scene generation with locally conditioned radiance fields. *Proc. ICCV*, 2021.
- [14] Ricson Cheng, Ziyang Wang, and Katerina Fragkiadaki. Geometry-aware recurrent neural networks for active visual recognition. *Proc. NeurIPS*, 31, 2018.
- [15] Hsiao-Yu Fish Tung, Ricson Cheng, and Katerina Fragkiadaki. Learning spatial common sense with geometry-aware recurrent networks. In *Proc. CVPR*, pages 2595–2603, 2019.
- [16] Vincent Sitzmann, Justus Thies, Felix Heide, Matthias Nießner, Gordon Wetzstein, and Michael Zollhöfer. Deepvoxels: Learning persistent 3d feature embeddings. In *Proc. CVPR*, 2019.
- [17] Stephen Lombardi, Tomas Simon, Jason Saragih, Gabriel Schwartz, Andreas Lehrmann, and Yaser Sheikh. Neural volumes: Learning dynamic renderable volumes from images. *Proc. SIGGRAPH*, 2019.
- [18] Ben Mildenhall, Pratul P Srinivasan, Matthew Tancik, Jonathan T Barron, Ravi Ramamoorthi, and Ren Ng. Nerf: Representing scenes as neural radiance fields for view synthesis. In *Proc. ECCV*, 2020.
- [19] Lior Yariv, Yoni Kasten, Dror Moran, Meirav Galun, Matan Atzmon, Basri Ronen, and Yaron Lipman. Multiview neural surface reconstruction by disentangling geometry and appearance. *Proc. NeurIPS*, 2020.
- [20] Ayush Tewari, Justus Thies, Ben Mildenhall, Pratul Srinivasan, Edgar Tretschk, Yifan Wang, Christoph Lassner, Vincent Sitzmann, Ricardo Martin-Brualla, Stephen Lombardi, et al. Advances in neural rendering. *Proc. Eurographics STAR*, 2021.
- [21] Vincent Sitzmann, Michael Zollhöfer, and Gordon Wetzstein. Scene representation networks: Continuous 3d-structure-aware neural scene representations. In *Proc. NeurIPS 2019*, 2019.

- [22] Alex Yu, Vickie Ye, Matthew Tancik, and Angjoo Kanazawa. pixelnerf: Neural radiance fields from one or few images. *Proc. CVPR*, 2020.
- [23] Wonbong Jang and Lourdes Agapito. Codenerf: Disentangled neural radiance fields for object categories. In *Proc. ICCV*, pages 12949–12958, October 2021.
- [24] Michael Niemeyer, Lars Mescheder, Michael Oechsle, and Andreas Geiger. Differentiable volumetric rendering: Learning implicit 3d representations without 3d supervision. In *Proc. CVPR*, pages 3504–3515, 2020.
- [25] Vincent Sitzmann, Semon Rezchikov, William T. Freeman, Joshua B. Tenenbaum, and Fredo Durand. Light field networks: Neural scene representations with single-evaluation rendering. In *Proc. NeurIPS*, 2021.
- [26] Shamit Lal, Mihir Prabhudesai, Ishita Mediratta, Adam W Harley, and Katerina Fragkiadaki. Coconets: Continuous contrastive 3d scene representations. In *Proc. CVPR*, pages 12487–12496, 2021.
- [27] Mehdi SM Sajjadi, Henning Meyer, Etienne Pot, Urs Bergmann, Klaus Greff, Noha Radwan, Suhani Vora, Mario Lucic, Daniel Duckworth, Alexey Dosovitskiy, et al. Scene representation transformer: Geometry-free novel view synthesis through set-latent scene representations. *Proc. CVPR*, 2021.
- [28] Alex Trevithick and Bo Yang. Grf: Learning a general radiance field for 3d scene representation and rendering. *Proc. ICCV*, 2020.
- [29] Adam R Kosiorek, Heiko Strathmann, Daniel Zoran, Pol Moreno, Rosalia Schneider, Soňa Mokrá, and Danilo J Rezende. Nerf-vae: A geometry aware 3d scene generative model. *Proc. ICML*, 2021.
- [30] Emilien Dupont, Miguel Bautista Martin, Alex Colburn, Aditya Sankar, Josh Susskind, and Qi Shan. Equivariant neural rendering. In *Proc. ICML*, pages 2761–2770. PMLR, 2020.
- [31] Xiao Fu, Shangzhan Zhang, Tianrun Chen, Yichong Lu, Lanyun Zhu, Xiaowei Zhou, Andreas Geiger, and Yiyi Liao. Panoptic nerf: 3d-to-2d label transfer for panoptic urban scene segmentation. *arXiv preprint arXiv:2203.15224*, 2022.
- [32] Eric R Chan, Connor Z Lin, Matthew A Chan, Koki Nagano, Boxiao Pan, Shalini De Mello, Orazio Gallo, Leonidas J Guibas, Jonathan Tremblay, Sameh Khamis, et al. Efficient geometry-aware 3d generative adversarial networks. In *Proc. CVPR*, pages 16123–16133, 2022.
- [33] Anpei Chen, Zexiang Xu, Andreas Geiger, Jingyi Yu, and Hao Su. Tensorf: Tensorial radiance fields. *arXiv preprint arXiv:2203.09517*, 2022.
- [34] Lingjie Liu, Jiatao Gu, Kyaw Zaw Lin, Tat-Seng Chua, and Christian Theobalt. Neural sparse voxel fields. In *Proc. NeurIPS*, 2020.
- [35] Christian Reiser, Songyou Peng, Yiyi Liao, and Andreas Geiger. Kilonerf: Speeding up neural radiance fields with thousands of tiny mlps. In *Proc. ICCV*, pages 14335–14345, 2021.
- [36] Alex Yu, Ruilong Li, Matthew Tancik, Hao Li, Ren Ng, and Angjoo Kanazawa. Plenotrees for real-time rendering of neural radiance fields. In *Proc. ICCV*, pages 5752–5761, 2021.
- [37] Songyou Peng, Michael Niemeyer, Lars Mescheder, Marc Pollefeys, and Andreas Geiger. Convolutional occupancy networks. In *Proc. ECCV*, 2020.
- [38] Adam W Harley, Zhaoyuan Fang, Jie Li, Rares Ambrus, and Katerina Fragkiadaki. A simple baseline for bev perception without lidar. *arXiv preprint arXiv:2206.07959*, 2022.
- [39] Jonah Philion and Sanja Fidler. Lift, splat, shoot: Encoding images from arbitrary camera rigs by implicitly unprojecting to 3d. In *Proc. ECCV*, pages 194–210. Springer, 2020.
- [40] Lennart Reiher, Bastian Lampe, and Lutz Eckstein. A sim2real deep learning approach for the transformation of images from multiple vehicle-mounted cameras to a semantically segmented image in bird’s eye view. In *2020 IEEE 23rd International Conference on Intelligent Transportation Systems (ITSC)*, pages 1–7. IEEE, 2020.
- [41] Thomas Roddick, Alex Kendall, and Roberto Cipolla. Orthographic feature transform for monocular 3d object detection. In *BMVC*, 2019.
- [42] Anh-Quan Cao and Raoul de Charette. Monoscene: Monocular 3d semantic scene completion. In *Proc. CVPR*, pages 3991–4001, 2022.

- [43] Jaebong Jeong, Janghun Jo, Sunghyun Cho, and Jaesik Park. 3d scene painting via semantic image synthesis. In *Proc. CVPR*, pages 2262–2272, June 2022.
- [44] Kaustubh Mani, Swapnil Daga, Shubhika Garg, Sai Shankar Narasimhan, Madhava Krishna, and Krishna Murthy Jatavallabhula. Monolayout: Amodal scene layout from a single image. In *Proc. CVPR*, pages 1689–1697, 2020.
- [45] Weixiang Yang, Qi Li, Wenxi Liu, Yuanlong Yu, Yuexin Ma, Shengfeng He, and Jia Pan. Projecting your view attentively: Monocular road scene layout estimation via cross-view transformation. In *Proc. CVPR*, pages 15536–15545, 2021.
- [46] Anthony Hu, Zak Murez, Nikhil Mohan, Sofia Dudas, Jeffrey Hawke, Vijay Badrinarayanan, Roberto Cipolla, and Alex Kendall. Fiery: Future instance prediction in bird’s-eye view from surround monocular cameras. In *Proc. CVPR*, pages 15273–15282, 2021.
- [47] Maciej Zięba, Marcin Przewięzlikowski, Marek Śmieja, Jacek Tabor, Tomasz Trzcinski, and Przemysław Spurek. Regflow: Probabilistic flow-based regression for future prediction. *arXiv preprint arXiv:2011.14620*, 2020.
- [48] Shaoyu Chen, Tianheng Cheng, Xinggang Wang, Wenming Meng, Qian Zhang, and Wenyu Liu. Efficient and robust 2d-to-bev representation learning via geometry-guided kernel transformer. *arXiv preprint arXiv:2206.04584*, 2022.
- [49] Yoni Kasten, Dolev Ofri, Oliver Wang, and Tali Dekel. Layered neural atlases for consistent video editing. *Proc. TOG*, 40(6):1–12, 2021.
- [50] Vickie Ye, Zhengqi Li, Richard Tucker, Angjoo Kanazawa, and Noah Snavely. Deformable sprites for unsupervised video decomposition. In *Proc. CVPR*, pages 2657–2666, 2022.
- [51] Zhipeng Bao, Pavel Tokmakov, Allan Jabri, Yu-Xiong Wang, Adrien Gaidon, and Martial Hebert. Discovering objects that can move. In *Proc. CVPR*, pages 11789–11798, 2022.
- [52] Zhixuan Lin, Yi-Fu Wu, Skand Vishwanath Peri, Weihao Sun, Gautam Singh, Fei Deng, Jindong Jiang, and Sungjin Ahn. Space: Unsupervised object-oriented scene representation via spatial attention and decomposition. In *Proc. ICLR*, 2020.
- [53] SM Eslami, Nicolas Heess, Theophane Weber, Yuval Tassa, David Szepesvari, Geoffrey E Hinton, et al. Attend, infer, repeat: Fast scene understanding with generative models. *Proc. NeurIPS*, 29, 2016.
- [54] Eric Crawford and Joelle Pineau. Spatially invariant unsupervised object detection with convolutional neural networks. In *Proc. AAAI*, 2019.
- [55] Adam Kosiorek, Hyunjik Kim, Yee Whye Teh, and Ingmar Posner. Sequential attend, infer, repeat: Generative modelling of moving objects. *Proc. NeurIPS*, 31, 2018.
- [56] Jindong Jiang, Sepehr Janghorbani, Gerard de Melo, and Sungjin Ahn. Scalable object-oriented sequential generative models. *Unknown Journal*, 2019.
- [57] Christopher P Burgess, Loic Matthey, Nicholas Watters, Rishabh Kabra, Irina Higgins, Matt Botvinick, and Alexander Lerchner. Monet: Unsupervised scene decomposition and representation. *arXiv preprint arXiv:1901.11390*, 2019.
- [58] Klaus Greff, Raphaël Lopez Kaufman, Rishabh Kabra, Nick Watters, Christopher Burgess, Daniel Zoran, Loic Matthey, Matthew Botvinick, and Alexander Lerchner. Multi-object representation learning with iterative variational inference. In *International Conference on Machine Learning*, 2019.
- [59] Klaus Greff, Antti Rasmus, Mathias Berglund, Tele Hao, Harri Valpola, and Jürgen Schmidhuber. Tagger: Deep unsupervised perceptual grouping. *Proc. NeurIPS*, 29, 2016.
- [60] Klaus Greff, Sjoerd Van Steenkiste, and Jürgen Schmidhuber. Neural expectation maximization. *Proc. NeurIPS*, 30, 2017.
- [61] Yilun Du, Shuang Li, Yash Sharma, B. Joshua Tenenbaum, and Igor Mordatch. Unsupervised learning of compositional energy concepts. In *Proc. NeurIPS*, 2021.
- [62] Cathrin Elich, Martin R. Oswald, Marc Pollefeys, and Joerg Stueckler. Weakly supervised learning of multi-object 3d scene decompositions using deep shape priors. *Computer Vision and Image Understanding*, 220:103440, 2022.

- [63] Chang Chen, Fei Deng, and Sungjin Ahn. Roots: Object-centric representation and rendering of 3d scenes. *JMLR*, 22:259–1, 2021.
- [64] Daniel Bear, Chaofei Fan, Damian Mrowca, Yunzhu Li, Seth Alter, Aran Nayebi, Jeremy Schwartz, Li F Fei-Fei, Jiajun Wu, Josh Tenenbaum, et al. Learning physical graph representations from visual scenes. *Proc. NeurIPS*, 33, 2020.
- [65] Sergey Zakharov, Wadim Kehl, Arjun Bhargava, and Adrien Gaidon. Autolabeling 3d objects with differentiable rendering of sdf shape priors. In *Proc. CVPR*, 2020.
- [66] Sergey Zakharov, Rares Andrei Ambrus, Vitor Campagnolo Guizilini, Dennis Park, Wadim Kehl, Fredo Durand, Joshua B Tenenbaum, Vincent Sitzmann, Jiajun Wu, and Adrien Gaidon. Single-shot scene reconstruction. In *Proc. CORL*, 2021.
- [67] Deniz Beker, Hiroharu Kato, Mihai Adrian Morariu, Takahiro Ando, Toru Matsuoka, Wadim Kehl, and Adrien Gaidon. Monocular differentiable rendering for self-supervised 3d object detection. In *Proc. ECCV*, pages 514–529. Springer, 2020.
- [68] Yilun Du, Kevin Smith, Tomer Ulman, Joshua B Tenenbaum, and Jiajun Wu. Unsupervised discovery of 3d physical objects from video. In *Proc. ICLR*, 2021.
- [69] Thu H Nguyen-Phuoc, Christian Richardt, Long Mai, Yongliang Yang, and Niloy Mitra. Blockgan: Learning 3d object-aware scene representations from unlabelled images. *Proc. NeurIPS*, 33:6767–6778, 2020.
- [70] Michael Niemeyer and Andreas Geiger. Giraffe: Representing scenes as compositional generative neural feature fields. In *Proc. CVPR*, pages 11453–11464, 2021.
- [71] Julian Ost, Fahim Mannan, Nils Thuerey, Julian Knodt, and Felix Heide. Neural scene graphs for dynamic scenes. In *Proc. CVPR*, 2021.
- [72] Bangbang Yang, Yinda Zhang, Yinghao Xu, Yijin Li, Han Zhou, Hujun Bao, Guofeng Zhang, and Zhaopeng Cui. Learning object-compositional neural radiance field for editable scene rendering. In *Proc. ICCV*, pages 13779–13788, October 2021.
- [73] Michelle Guo, Alireza Fathi, Jiajun Wu, and Thomas Funkhouser. Object-centric neural scene rendering. *arXiv preprint arXiv:2012.08503*, 2020.
- [74] Bangbang Yang, Yinda Zhang, Yijin Li, Zhaopeng Cui, Sean Fanello, Hujun Bao, and Guofeng Zhang. Neural rendering in a room: Amodal 3d understanding and free-viewpoint rendering for the closed scene composed of pre-captured objects. *arXiv preprint arXiv:2205.02714*, 2022.
- [75] Yinyu Nie, Xiaoguang Han, Shihui Guo, Yujian Zheng, Jian Chang, and Jian Jun Zhang. Total3dunderstanding: Joint layout, object pose and mesh reconstruction for indoor scenes from a single image. In *Proc. CVPR*, pages 55–64, 2020.
- [76] Jonathan T Barron, Ben Mildenhall, Dor Verbin, Pratul P Srinivasan, and Peter Hedman. Mip-nerf 360: Unbounded anti-aliased neural radiance fields. *Proc. CVPR*, 2021.
- [77] Yiheng Xie, Towaki Takikawa, Shunsuke Saito, Or Litany, Shiqin Yan, Numair Khan, Federico Tombari, James Tompkin, Vincent Sitzmann, and Srinath Sridhar. Neural fields in visual computing and beyond. *Computer Graphics Forum*, 2022.
- [78] Thomas Neff, Pascal Stadlbauer, Mathias Parger, Andreas Kurz, Joerg H Mueller, Chakravarty R Alla Chaitanya, Anton Kaplanyan, and Markus Steinberger. Donerf: Towards real-time rendering of compact neural radiance fields using depth oracle networks. In *Computer Graphics Forum*. Wiley Online Library, 2021.
- [79] Daniel Rebain, Mark Matthews, Kwang Moo Yi, Dmitry Lagun, and Andrea Tagliasacchi. Lolnerf: Learn from one look. In *Proc. CVPR*, pages 1558–1567, 2022.
- [80] Nishchal Bhandari. *Procedural synthetic data for self-driving cars using 3D graphics*. PhD thesis, Massachusetts Institute of Technology, 2018.